https://doi.org/10.5194/nhess-2022-255
Preprint. Discussion started: 14 December 2022
© Author(s) 2022. CC BY 4.0 License.

Natural Hazards and Earth System Sciences
Open Access
Discussions

Comparison of two nationwide lightning location systems and characteristics of could-to-ground lightning in China

Ruijiao Jiang[a], Guoping Zhang[a,*], Shudong Wang[a], Bing Xue[a], Zhengshuai Xie[b], Tingzhao Yu[a], Kuoyin Wang[a], Jin Ding[a], Xiaoxiang Zhu[a]

[a] Public Meteorological Service Center, China Meteorological Administration, Beijing 100081, China

[b] Weather Modification Centre, China Meteorological Administration, Beijing 100081, China

[*] Corresponding author. E-mail address: zhanggp@cma.gov.cn

Abstract

The lightning location system based on multiple sub-stations is an effective means of lightning observation. This study first compares the two nationwide lightning location systems in China, the Advanced TOA and Detection System (ADTD) and the Three-Dimensional Lightning Location System (3D-LLS), using the observations in 2020. As a significantly updated version of ADTD, 3D-LLS has a cloud-to-ground (CG) detection efficiency of nearly twice ADTD. However, its scarce distribution sites in central Tibet, western Xinjiang, eastern Qinghai, and eastern Heilongjiang account for some blind observation areas where ADTD could play a supplementary role. The ratio of +CG and the distribution of currents indicate that 3D-LLS misjudges a certain number of intracloud (IC) pulses as return strokes. Besides, the IC detection developed by 3D-LLS is still inefficient. In the results, the IC flashes only account for half of CG flashes, much smaller than the regular ratio (twice). According to the comparison with the nearly no-miss optical observations in Guangzhou, the CG detection efficiency of ADTD and 3D-LLS herein is 24.5% and 50.5%. Further improvements are expected in terms of the above shortages. Still, the ground-based observation has better detection efficiency and accuracy than the satellite, especially for CG lightning. The dataset from ADTD in 2016-2021 is employed to analyze the lightning characteristics' temporal and spatial distributions and the difference between +CG and -CG over China. It can be concluded that low latitude, undulating terrain, seaside, and humid surface are favorable factors for lightning occurrence. Thus the southeast coastland has the largest lightning density, while the northwest deserts and basins and the western and northern Tibetan Plateau have almost no lightning. For the period with high CG frequency (summer of a year or afternoon of a day), the ratio of +CG and the discharge intensity is relatively small. The Tibetan Plateau leads to the complexity of lightning activity in China and lays the foundation for studying the impact of surface elevation on lightning. Results indicate that the +CG ratio on the eastern and southern plateau is up to 15%, and the west and north sides have a low percentage. The discharge intensity of +CG and -CG on the Tibetan Plateau is approximate, while the +CG always has a larger current than

https://doi.org/10.5194/nhess-2022-255
Preprint. Discussion started: 14 December 2022
© Author(s) 2022. CC BY 4.0 License.

-CG on the plains.

Keywords: China, ADTD, 3D-LLS, Comparison, Lightning characteristics, +CG

1. Introduction

Most lightning is generated mainly through meso-small scale severe convective weather, with few occurring in stratus clouds and tropical cyclones and occasionally during volcanic eruptions, nuclear explosions, and dust storms (Rakov and Uman, 2003). Lightning, a violent long-distance transient discharge phenomenon, could cause severe disasters such as human and animal casualties, forest fires, and electronic and communication equipment interruptions. Therefore advanced lightning monitoring technology is necessary for the development of lightning science and also scientific protection against lightning disasters.

Lightning discharge emits electromagnetic spectrums with a broad range, providing an essential avenue for lightning detection. The very low frequency / low frequency (VLF/LF, 20-300 kHz) band radiation is mainly produced by the cloud-to-ground (CG) return strokes, intracloud (IC) K-changes, and other discharge processes with a large spatial scale. VLF/LF electromagnetic waves could propagate along the ground surface or be reflected between the surface and ionosphere propagation, with superiority of long propagation distance (hundreds to thousands of kilometers) and slow attenuation. This frequency range thus is suitable for large-scale lightning detection and is currently the most commonly used target detection band for ground-based lightning location systems.

Representative examples of modern lightning location systems working in VLF/LF band are mainly the U.S. National Lightning Detection Network (NLDN), Los Alamos Sferic Array (LASA), European Cooperation for Lightning Detection (EUCLID), etc. The three nationwide detection networks in China are the Advanced TOA and Detection System (ADTD) operated by the Meteorological Observation Centre of China Meteorological Administration (CMA), the Lightning Location System (LLS) of the State Grid Corporation of China, and the Three-Dimensional Lightning Location System (3D-LLS) deployed by the Institute of Electrical Engineering of Chinese Academy of Sciences (CAS). There are also small-scale and refined detection systems in local areas, such as the Beijing Lightning Network (BLNET) established by the Institute of Atmospheric Physics of CAS, the Guangdong-Hongkong-Macao Lightning Location System (GHMLLS) deployed by the meteorological departments of Guangdong Province, Hongkong, and Macao.

Due to the differences in equipment types, instrument errors, calculation principles, and installation environments, there are certain deviations in the detection results of different lightning location systems. To improve the reliability, effective utilization rate, and practical application effect of the systems, and also to provide a theoretical basis for the optimization of future networking efficiency and the fusion of multi-source

https://doi.org/10.5194/nhess-2022-255
Preprint. Discussion started: 14 December 2022
© Author(s) 2022. CC BY 4.0 License.

lightning location data, it is crucial to evaluate and analyze the quality of the networks. Currently, there are two dominant methods for assessing lightning location systems. One is to use a limited number of rocket-triggered lightning cases and lightning current measurement data or optical image data of high structures as references to statistically evaluate the current or location deviation (Jerauld et al., 2005; Nag et al., 2011; Schulz et al., 2016). Another way is the comparison between different systems (Bitzer and Burchfield, 2016; Murphy and Said, 2020; Srivastava et al., 2017). The former gives more accurate assessment results but is only available when the striking location can be confirmed by other sources. For vast observation areas, the assessment of detection accuracy and efficiency can only be obtained by comparing networks, often using one with known better performance to assess another. If the detection efficiency (DE) of both systems has not been evaluated before, a Bayesian algorithm can be used to find the relative DE (Bitzer and Burchfield, 2016; Bitzer et al., 2016).

China spans a wide range of latitudes from north to south and significant terrain changes from east to west, and the western and northern parts of the Tibetan Plateau have large uninhabited areas with altitudes above 4500 m. The above factors pose challenges for the installation of lightning detectors and the improvement of the accuracy of locating algorithms. Among the three nationwide systems, only ADTD and 3D-LLS are available for us. In reviewing the literature, comparative evaluation of these two networks is lacking and mainly aimed at localized areas. In this paper, we use the nationwide CG data in 2020 obtained from ADTD and 3D-LLS to compare their capabilities in terms of lightning density, time difference, relative positioning accuracy, and current peak value. The consequences could assess the quality and reliability of the two datasets and their application in different scenarios. In addition, China's wide latitude and longitude range and complex topography make for studying the relationship between lightning and geographic factors. This study makes use of ADTD data from 2016-2021 to analyze lightning distribution in China and the temporal and spatial distribution difference between +CG and -CG.

2. Comparison of ADTD and 3D-LLS

2.1 Introduction to the two networks

ADTD was first developed by the National Space Science Center (NSSC) of CAS in 2007 and is currently operated by the Meteorological Observation Centre of CMA. The system consisted of 435 sub-stations (by 2020) equipped with lightning detectors and the central data processing station deployed at the National Meteorological Information Center. ADTD can generally achieve nationwide detection without blind areas and is nowadays the most widely used system by the meteorological departments in China.

3D-LLS has been in operation by the Institute of Electrical Engineering of CAS since 2013, which is an upgraded version of the equipment and algorithm of ADTD,

https://doi.org/10.5194/nhess-2022-255
Preprint. Discussion started: 14 December 2022
© Author(s) 2022. CC BY 4.0 License.

adding the function of detecting IC lightning and improving the efficiency of CG lightning. 3D-LLS also went on to scale over 400 sub-stations by 2020, but thick distributed in southern and eastern China and sparsely in western China. Part of the station distribution in 2018 can be found in Wang et al. (2020). 3D-LLS has also expanded to other Asian countries such as Sri Lanka, Myanmar, Cambodia, and Korea.

A time-of-arrival (TOA) technique with a GPS timing error of fewer than 20 ns (clear sky) is used by both two networks, and the detecting targets are the VLF/LF pulses of CG return strokes (and IC K-changes). A lightning flash might comprise several CG strokes or IC K-changes, and both systems group single-point signals to a flash event according to their separation in time and space. However, their rules of categorization are different, as ADTD classified the return strokes within 500 ms time interval and 10 km distance interval as a single CG flash, while 3D-LLS set the thresholds as 1 s and 10-30 km to group a single CG or IC flash and distinguished the two types by the discharge height. This is one factor leading to the inconsistency in the number of lightning flashes between the two networks.

In this study, ADTD and 3D-LLS datasets were downloaded from the CMA big data cloud platform. Time of occurrence, latitude, longitude, current peak value, number of located stations, (type of lightning) for each flash was obtained.

2.2 Comparison of detection results

Since 3D-LLS had been adding sub-stations until 2020, this research only used the data in 2020 to compare the performance of the two networks. As 3D-LLS only retained lightning detected by five or more stations simultaneously this year, accordingly, this study did the same for ADTD data. Therefore, the retained cases were highly reliable, but it led to some missing cases where stations are sparse.

In 2020, ADTD detected a total of 5,898 thousand CG flashes in China, in which +CG flashes accounted for 8.5%. 3D-LLS detected 10,464 thousand CG flashes, with a DE nearly twice that of ADTD and a +CG flash percentage of 21.4%. In addition, 3D-LLS also detected 4,250 thousand IC flashes. In general, IC flashes account for 2/3 of the total number of lightning flashes (Rakov and Uman, 2003). It can be inferred that the missed rate for IC is greater than CG, as the discharge intensity of IC K-change is much smaller than that of CG stroke, which is also the technical bottleneck of most ground-based lightning location systems at present.

In our previous study, we calculated the lightning density in the vicinity of the Canton Tower in Guangdong using optical observation by the Tall-Object Lightning Observatory in Guangzhou (TOLOG), which is currently regarded as a nearly no-miss observation (Wu et al., 2019; Jiang, 2021). The result was that the CG flash density was 20 km^{-2} yr^{-1} within a 3 km radius of the Canton Tower. The detection results in the same region for ADTD and 3D-LLS are 4.9 km^{-2} yr^{-1} and 10.1 km^{-2} yr^{-1}, respectively. The DE of the two networks correspondingly is only 24.5% and 50.5%, and improvement is expected.

For further comparison, China's land area is divided into a 0.25°×0.25° grid

https://doi.org/10.5194/nhess-2022-255
Preprint. Discussion started: 14 December 2022
© Author(s) 2022. CC BY 4.0 License.

according to the latitude and longitude, and the annual CG flash density is calculated for each grid. Fig. 1(a,b) shows the distribution results of ADTD and 3D-LLS in 2020. Due to the huge regional differences, an exponential color scale is used here, with regions of high density indicated by red and regions of low indicated by blue, with a transition color in between. The overall distribution of the two networks is similar, and the high-value and low-value regions correspond well. The specific distribution characteristics will be detailed in section 3.1.

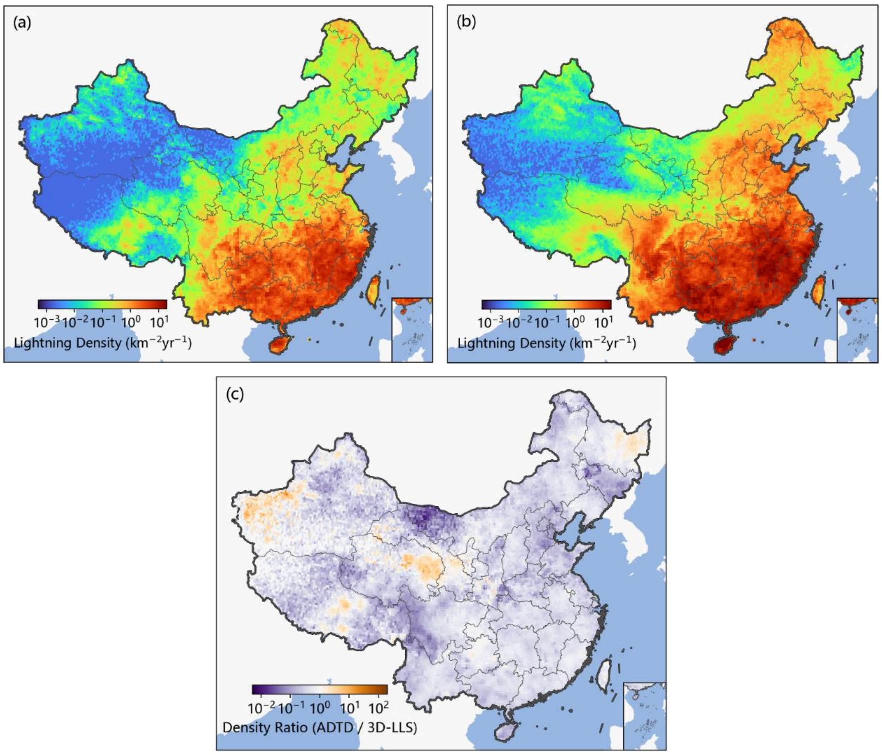

Fig. 1. Distribution of CG flash in China detected by (a) ADTD and (b) 3D-LLS in 2020; (c) ratio of CG flashes detected by the two networks in 2020 (ADTD/3D-LLS). The grid size is 0.25°×0.25°, and the map is in Lambert's equirectangular cone projection, the same below.

The distribution of DE difference is shown in Fig. 1(c), calculated by dividing the grid densities of the two systems (ADTD/3D-LLS). When their DE is similar, it is represented by white; when the DE of ADTD is higher, it is represented by brown; when the DE of 3D-LLS is higher, it is represented by purple. The darker color corresponds to the bigger difference. The DE difference between the two systems can be up to a hundred times. In general, 3D-LLS has a higher DE as been significantly upgraded, but its site distribution is relatively uneven. It is particularly dense in some parts of Yunnan, Sichuan, Tibet, Inner Mongolia, Hebei, Jilin, etc. Thus the DE of these regions is high. In contrast, the number of stations deployed in central Tibet, western Xinjiang, eastern

Qinghai, eastern Heilongjiang, etc., is scarce, even leading to some blind detection areas. Overall, the DE of 3D-LLS is about two times that of ADTD.

The current peak value of CG detected by the two networks is compared (removing outliers above ±300 kA), as shown in Fig. 2, with the orange histogram representing ADTD and the slash histogram representing 3D-LLS. Most of the lightning discharged with the current peak between -100 kA and 100 kA. The negative currents measured by ADTD are generally larger than 3D-LLS, with an average ratio of 1.46. For +CG, the current peak distributions of ADTD and 3D-LLS are approximately the same when the value is greater than 30 kA, with a ratio of 1.03. However, 3D-LLS has a large number of outliers in the 0-30 kA range, which is presumed to result from misclassifying IC as +CG, leading to a high percentage of +CG of 21.4%. This phenomenon is mostly because that 3D-LLS distinguished IC and CG by the height of the radiation source. According to the principle of the TOA algorithm, the positioning error in the vertical direction is much larger than that in the horizontal direction, so a significant number of misjudgment cases appeared. Merge the electric field waveform identification to the discrimination algorithm might help to improve the recognition accuracy. ADTD had already eliminated the +CG with a current peak of 0-10 kA from the original data to reduce misjudgment.

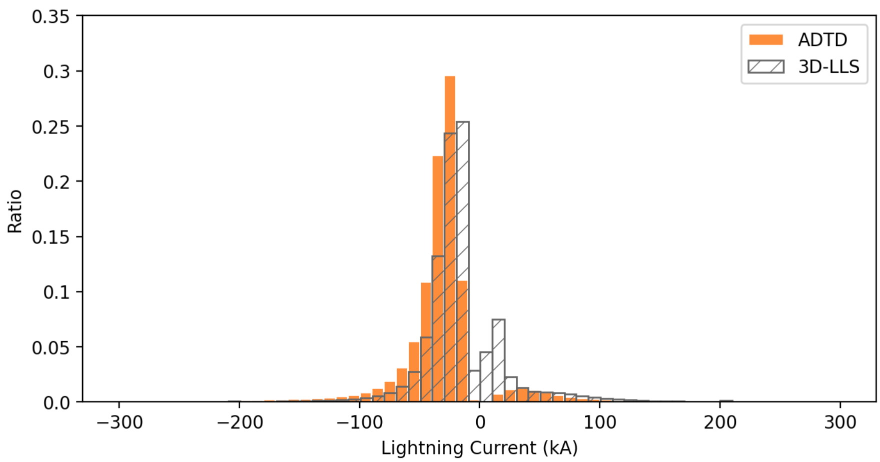

Fig. 2. Distribution of current peak value of CG flashes detected by the two networks in 2020

2.3 Match of the same CG flash from two datasets

Comparing the detection results for the same radiation source is necessary for valuing the difference between the two networks. The spatial and temporal thresholds for matching vary between studies, with most having a time difference (Δt) threshold of a few hundred ms and a spatial distance (Δr) threshold of 10-30 km (0.1 ms & 1 km (Pohjola and Mäkelä, 2013), 1 s & 15 km (Poelman et al., 2013), 200 ms & 20 km (Bitzer and Burchfield, 2016), etc.). Different matching thresholds bring differences to the results. In our study, when the Δt threshold is set to be 1 s, 3,219 thousand CG

https://doi.org/10.5194/nhess-2022-255
Preprint. Discussion started: 14 December 2022
© Author(s) 2022. CC BY 4.0 License.

flashes are matched if the Δr threshold is set to be 30 km, and the match number is 3,079 thousand if the Δr threshold is set to be 10 km. It means the Δr threshold has no significant effect on the matching results, and the number of matched CG flashes is about 60% in ADTD and 30% in 3D-LLS. The percentages imply that even though the DE of 3D-LLS has been improved a lot, a large number of flashes is still undetected. By expanding the Δt distribution in the 0-1 s interval, it can be found that Δt is evenly distributed in the 20 μs-1 s interval, while a large proportion of Δt in the 0-20 μs (0.002% of 1 s) interval, as shown in Fig. 3(a). There are 64 thousand (1.1% of CG flashes by ADTD, 0.6% of CG flashes by 3D-LLS) flashes with Δt in 0-20 μs, and the corresponding Δr distribution is shown in Fig. 3(b), with 86.5% within 2 km and 96.8% within 4 km. It is reasonable to assume that these radiation sources came from the same lightning strokes recorded by two systems. Bitzer and Burchfield (2016) indicated that the Δt of the same stroke by different networks should be no more than 50 μs in case they are timed by GPS. The two networks have different criteria for grouping flashes, and if there was a missed stroke in a lightning flash and they did not use the same stroke to represent the flash, the same lightning flash could not be matched in this case, leading to the low matching ratio.

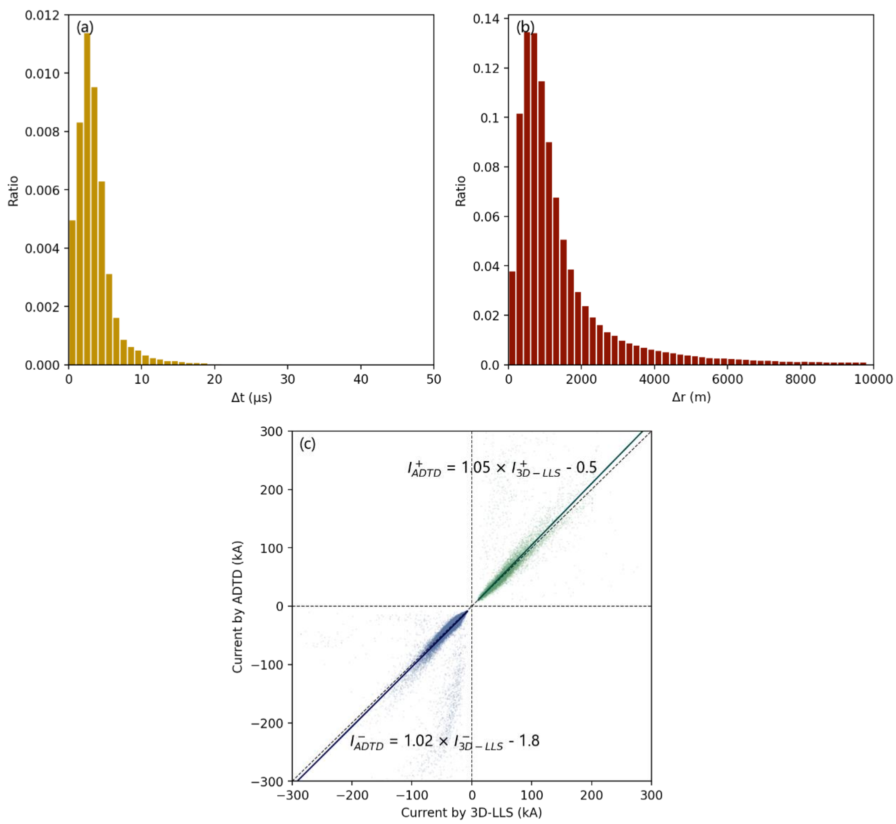

https://doi.org/10.5194/nhess-2022-255
Preprint. Discussion started: 14 December 2022
© Author(s) 2022. CC BY 4.0 License.

Fig. 3. Difference between the matched lightning stroke of the two systems. (a) Δt distribution; (b) Δr distribution; (c) current comparison, green represents +CG, and blue represents -CG, same below.

The same stroke currents detected by the two systems are compared, and +CG and -CG are indicated by different colors, as shown in Fig. 3(c). For most of the strokes, the current measurements are very close. However, there are some anomalies that the ADTD currents are significantly higher than the 3D-LLS currents. By examining the locations of these points, they are concentrated within a 50 km radius of the junction of Guizhou, Guangxi, and Hunan. Since there is no special feature in this area, it is inferred that some ADTD sub-stations might work abnormally. After eliminating these anomalies, the currents of +CG and -CG are fitted, respectively, and the relationship is marked in Fig. 3(c) with r^2 of 0.90 and 0.81. The current ratios after matching strokes are more accurate than the generalized current ratios calculated in Section 2.2. By matching and fusing the detection results of the two systems, the advantages can be well complemented, and the existing resources can be fully exploited to achieve further optimization of existing equipment.

3. CG characteristics of China

Although the DE of ADTD is less than that of 3D-LLS in the areas with dense site distribution, ADTD has a relatively more uniform site placement and a smaller blind spot range. Moreover, the available years of 3D-LLS are short, and the misjudgment of +CG is common. Therefore, the ADTD dataset from 2016-2021 is utilized to analyze China's lightning characteristics. The data are filtrated by the number of triggered stations (⩾3). Positive strokes with small peak currents (<10 kA) are likely to be misclassified as CG discharges when those are more likely to be of intracloud nature (Cummins et al., 1998), so they are discarded from the dataset.

3.1 CG distribution in China

Fig. 4 showed the surface height distribution of China based on the global surface elevation data (resolution of 30 m) from NASA's new generation earth observation satellite, Terra. The large latitudinal span, the great terrain disparity, and the complex topography varied the climate features in China. As a fundamental meteorological element, lightning mainly occurs in meso-small scale thunderstorms, and its long-time accumulation characteristics are closely associated with the climate of China. Atmospheric circulation, topography, distance from the sea, latitude, etc., jointly determine the terrestrial spatial distribution of lightning in China.

https://doi.org/10.5194/nhess-2022-255
Preprint. Discussion started: 14 December 2022
© Author(s) 2022. CC BY 4.0 License.

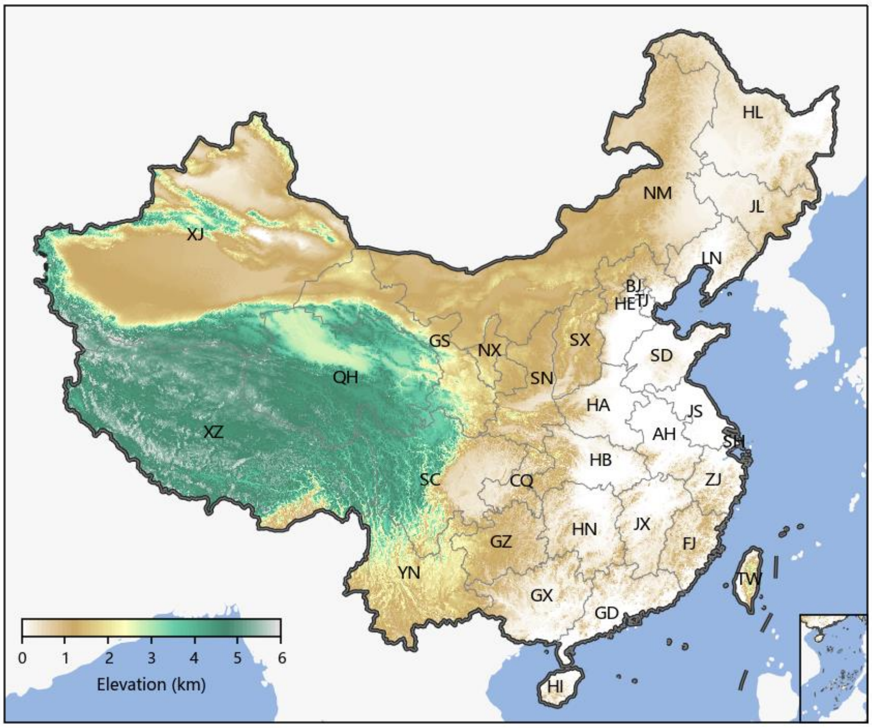

Fig. 4. Altitude distribution map of China with the location of each province and municipality (indicated by abbreviations, for details, refer to：*https://www.iso.org/obp/ui/#iso:code:3166:CN*）

China can be divided into four major geographical regions, namely, southern China (Region-I), northern China (Region-II), northwestern China (Region-III), and the Qinghai-Tibet region of China (Region-IV), as shown in Fig. 5. Qinling Mountains-Huaihe River line (roughly coinciding with the 0 ℃ isotherms and 800 mm annual precipitation line in January) is the dividing line between Region-I and Region-II. The Daxing’an Mountains-Yinshan Mountains-Helan Mountains (dividing monsoon and non-monsoon and the 400 mm annual precipitation line) is the boundary between Region-II and Region-III. The dividing line between Region-IV and Region-I-II-III is roughly the line between China's terrain's first and second steps.

Fig. 5 shows the annual average CG flash density distribution from 2016-2021. Most CG flashes are concentrated in Region-I with a density greater than 1 km^{-2} yr^{-1}. The leap line of lightning density corresponds well with the 0 ℃ isotherms in January, the 800 mm annual equivalent precipitation line, and the eastern dividing line of the first and second terrain steps. The climate in Region-I is mainly influenced by the tropical\subtropical monsoon. The southeast monsoon from the Pacific Ocean and the southwest monsoon from the Indian Ocean makes the summer hot and humid and prone to thunderstorms. In particular, the monsoon influence is more pronounced in the coastal areas with abundant water vapor and thermal conditions. In the mountainous

https://doi.org/10.5194/nhess-2022-255
Preprint. Discussion started: 14 December 2022
© Author(s) 2022. CC BY 4.0 License.

regions of Hainan, Guangdong, Fujian, and Zhejiang, where the rolling topography lifts the warm and humid air masses, thunderstorm activity is most frequent, so the lightning density is especially high. Although the Sichuan Basin and Yunnan are far from the coastline, they are located at the eastern and southern windward slopes of the Tibetan Plateau, which benefits the generation of thunderstorm activities due to the topographic uplift.

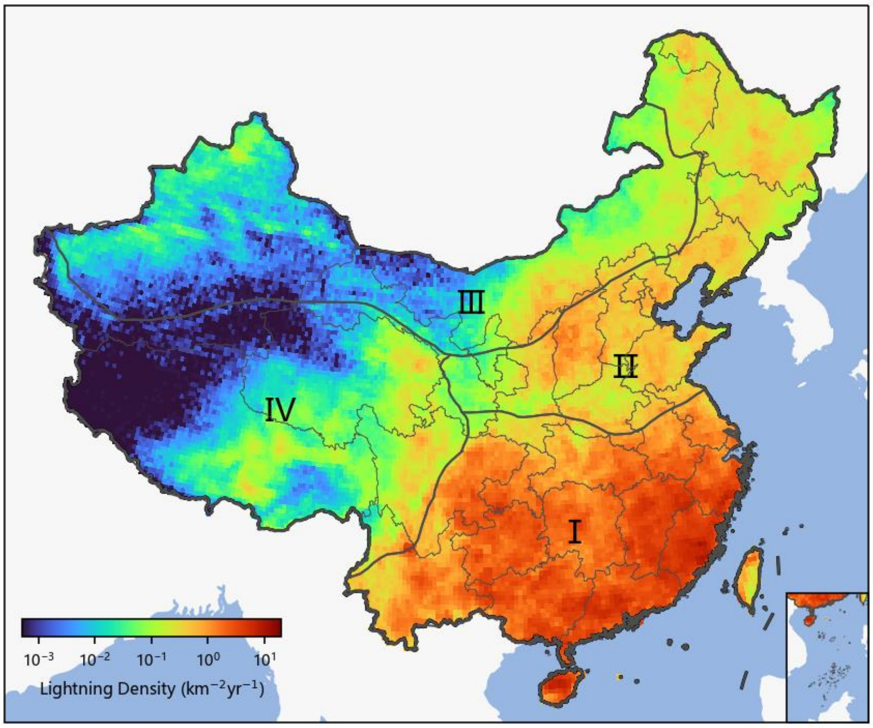

Fig. 5. 2016-2021 annual average CG flash density distribution in China (Region-I: southern China; Region-II: northern China; Region-III: northwestern China; Region-IV: Qinghai-Tibet region of China)

Region-II has mainly the temperate monsoon climate, with summer influenced by the southeast monsoon carrying temperate marine air mass or degenerate tropical marine air mass, making summer warm and rainy. Most areas have CG flash density between 0.1-1 km^{-2} yr^{-1}, slightly lower than Region-I. The lightning density in Region-II is also greater in the seaside area than inland areas. Shanxi is located in mountainous region, and the undulating terrain makes it a high incidence area for thunderstorm activity. Region-II has the most extensive plain, Northeastern China Plain, which is in the shape of a trumpet, surrounded by the Daxing'an Mountains-Xiaoxing'an Mountains-Changbai Mountains. The landform is conducive to the southeast monsoon to reach the inland areas of Region-II and form summer thunderstorms. Jilin is only a dozen kilometers from the Sea of Japan, facilitating the entry of Japanese warm air

https://doi.org/10.5194/nhess-2022-255
Preprint. Discussion started: 14 December 2022
© Author(s) 2022. CC BY 4.0 License.

currents. Therefore, thunderstorm activity is relatively intense in Region-II despite its high latitude.

Region-III, including Xinjiang, northern Gansu, and most of Inner Mongolia, has a temperate continental climate. The southern and central parts of Region-III are mostly vast deserts and gobies. The Tibetan Plateau blocks the humid South Asian monsoon, and its arid surface cannot produce abundant water vapor, so almost no thunderstorms are generated here. Although the Tianshan Mountains, Kunlun Mountains, Altay Mountains, and Tarbahatai Mountains in Region-III are located in the hinterland of the Eurasian continent, they are still provided with water vapor for thunderstorm generation from the westerly circulation transporting evaporated water vapor from the Atlantic Ocean and the Eurasian continent, making the northern mountainous areas occupy almost all the lightning activity in Xinjiang. The southeastern monsoon flowing through Region-II, reaching the eastern and central mountainous regions in Inner Mongolia in summer, can still bring some thunderstorm processes.

The main body of Region-IV is the Tibetan Plateau, mainly including Tibet, Qinghai, southern Xinjiang, and western Sichuan. It has a highland mountain climate, and the overall geomorphic distribution trend is increasing from west to east (Ma et al., 2021). The uninhabited areas above 4500 m in elevation in the west and north of Region-IV are icy all year round, covered by snows and glaciers. The Qaidam Basin in Qinghai is a closed, huge interrupted basin, with dry sinking airflow from the northern edge of the plateau in summer, leading to water shortage. There are few thunderstorm activities in the areas mentioned above, and the distribution of sub-stations is sparse, making them the regions with the lowest lightning density detected in China, with CG flash density less than 10^{-3} km^{-2} yr^{-1}. The eastern Himalayas, near the Yarlung Tsangpo River Grand Canyon, has relatively low altitude, opening a "gap" for the influx of abundant water vapor from the Bay of Bengal. The rapid climb of water vapor leads to frequent thunderstorms. The thunderstorms around Nagqu in the central part of the plateau are mainly located between the east-west Himalayas Mountains and Tanggula Mountains. The thunderstorms on the east side of the plateau are mainly influenced by the low vortex and the shear line, which is usually stable at around 32.5 °N. The high lightning density area is located precisely on the south side of the shear line.

The annual average CG flash density of each province and municipality is calculated and ranked in Fig. 6, and their geographical locations are shown in Fig. 4. Among them, Fujian (FJ) has the leading average CG flash density with more than 4.5 km^{-2} yr^{-1}, followed by Hainan (HI), Zhejiang (ZJ), Jiangxi (JX) and Guangdong (GD) with more than 3 km^{-2} yr^{-1}. Guangxi (GX) and Guizhou (GZ) have a density of around 2.5 km^{-2} yr^{-1}, while other inland provinces in Region-I are less than 2 km^{-2} yr^{-1}. The density of Shanxi (SX) in Region-II is the highest, close to 1 km^{-2} yr^{-1}. In the other provinces and municipalities in Region-II, Henan (HA), Shaanxi (SN), Hebei (HE), Beijing (BJ), Shandong (SD), Tianjin (TJ), Heilongjiang (HL), and Liaoning (LN) have the close value between 0.2-0.4 km^{-2} yr^{-1}. The density in Ningxia (NX), Qinghai (QH), Gansu (GS), Tibet (XZ), and Xinjiang (XJ) in Region-III and Region-IV is the lowest

https://doi.org/10.5194/nhess-2022-255
Preprint. Discussion started: 14 December 2022
© Author(s) 2022. CC BY 4.0 License.

in China, which is less than 0.1 km^{-2} yr^{-1}.

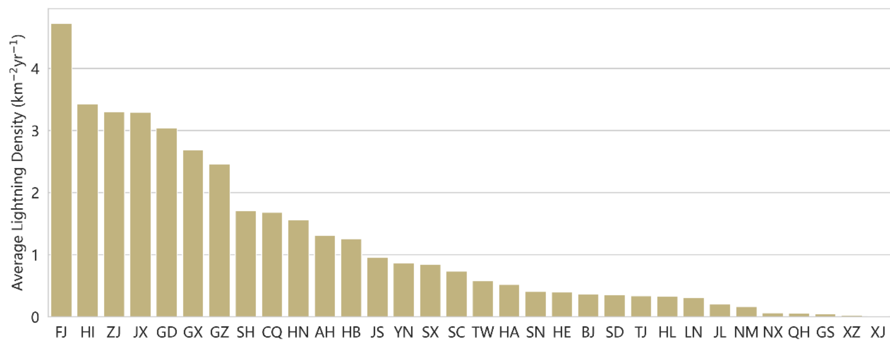

Fig. 6. Comparison and ranking of annual average CG density by province and municipality

3.2 Differences between +CG and -CG

According to the different polarities of neutralized charge in thunderclouds, CG can be divided into +CG and -CG. Compared with -CG, +CG generally has a lower probability of occurrence, only about 10%, but has a larger spatial scale and charge transfer, resulting in a more robust hazard (Preston and Tolver, 1989). Much work has been done on the comparative study of +CG and -CG in local areas (Nag et al., 2014; Rakov and V., 2003), and on their basis, this study further analyzes the spatial and temporal variability of +CG and -CG in China with the complex climatic and geographical factors.

3.2.1 Comparison of the temporal distribution of +CG and -CG

Fig. 7(a) shows the monthly average CG flash frequency distribution for six years from 2016-2021 in China. The frequency fluctuates significantly in different months, with the most frequent occurrence in August (-CG flashes up to 1,345 thousand and +CG flashes up to 152 thousand). December has the least number, with only 5 thousand -CG flashes and less than 400 +CG flashes. Lightning activity is also rare in November, January, and February, with an abrupt jump in March and a transitional increase in subsequent months. According to the seasonal classification, lightning activity is most active in summer (June, July, and August), accounting for 70.7% of the year. In other seasons, lightning is more frequent in spring (19.1%) than in autumn (9.8%) but much less than in summer. The main reason is that the summer monsoon affecting China has started to form during April and May, while the cold and dry winter monsoon starts to build up and push southward from September, making thunderstorm activity in spring and autumn mainly concentrated in southern areas, especially coastal areas. In winter, China's mainland is controlled primarily by cold high pressure, when there is very little lightning in most regions and only a small amount of lightning occurs in the southeastern coastal areas, accounting for only 0.4% of all year round. Overall, the seasonal trend is that the lightning distribution advances from south to north and then

https://doi.org/10.5194/nhess-2022-255
Preprint. Discussion started: 14 December 2022
© Author(s) 2022. CC BY 4.0 License.

retreats southward, which is consistent with the trend of the summer monsoon. In addition, the proportion of +CG flashes in different months is calculated, indicated by the gray line in Fig. 7(a). The proportion of +CG flashes and the lightning frequency have an obvious inverse trend. The proportion of +CG is low, less than 10%, in the months with frequent lightning. In contrast, the ratio is very high in winter, when thunderstorms are not easily generated, even up to more than 40% in December.

The current peak value of the two types of CG flashes in different months is analyzed, as shown in Fig. 7(b). On the whole, the distribution range is wider in winter than in other seasons. The average of each month is shown by the white cross in the figure and the variation trends by red lines. From the results, the discharge intensity of +CG flashes is greater than -CG flashes. The current of +CG and -CG flashes is the largest in January and December. The difference between -CG flashes is not obvious in other months, while the intensity of +CG flashes has an obvious trough in August. The discharge intensity and the proportion of +CG flashes have similar trends, with a higher proportion and stronger discharge intensity in winter and a lower proportion and weaker discharge intensity in summer.

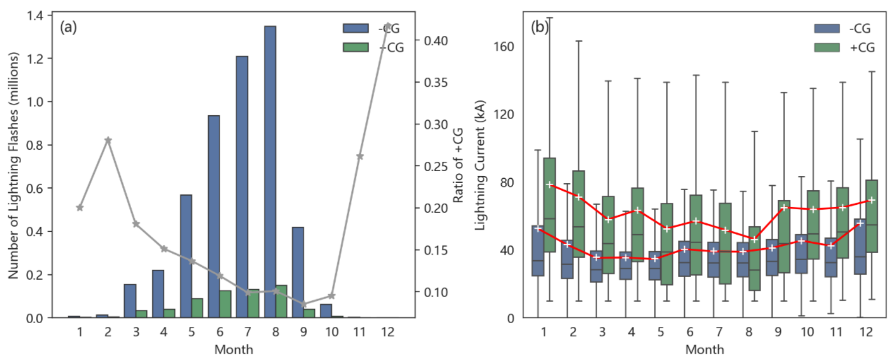

Fig. 7. Seasonal variation of (a) frequency and (b) discharge intensity of +CG and -CG flash. The gray line in (a) represents the percentage of +CG flashes, the red line in (b) represents the average current of each month, and the -CG flash currents are expressed in absolute values, the same below.

In addition, the hour-by-hour frequency and intensity variations of the two types of CG during the day are shown in Fig. 8. The frequency of +CG and -CG flashes has obvious fluctuation during the day. The variation trend of +CG and -CG is consistent, and the active period is mainly concentrated in the late afternoon to midnight. Most of the summer thunderstorms in China derive from thermal effects. The solar zenith angle rises after noon, radiative heating keeps enhancing, thermal conditions become abundant and conducive to the development of convection, and lightning activity is gradually activated. With the accumulation of water vapor, lightning frequency peaks at 17:00. After nightfall, following the weakening of thermal conditions and unstable energy, the lightning decreases continuously and drops to a low at 11:00 the next day. The proportion of +CG flashes is inversely correlated with the amount of CG flashes, but the phase difference lags 1-2 h. The ratio of +CG flashes is highest at 10:00, above

https://doi.org/10.5194/nhess-2022-255
Preprint. Discussion started: 14 December 2022
© Author(s) 2022. CC BY 4.0 License.

15%, and lowest at 15:00, only 2%, with two sub-peaks at 22:00 and 6:00, respectively.

The current distribution and average of +CG and -CG flashes are shown in Fig. 8(b). The daily variation is not apparent. The current intensity is slightly lower from 12:00 to 19:00 in the afternoon, and the lowest point is at 14:00, while the other periods are relatively stable.

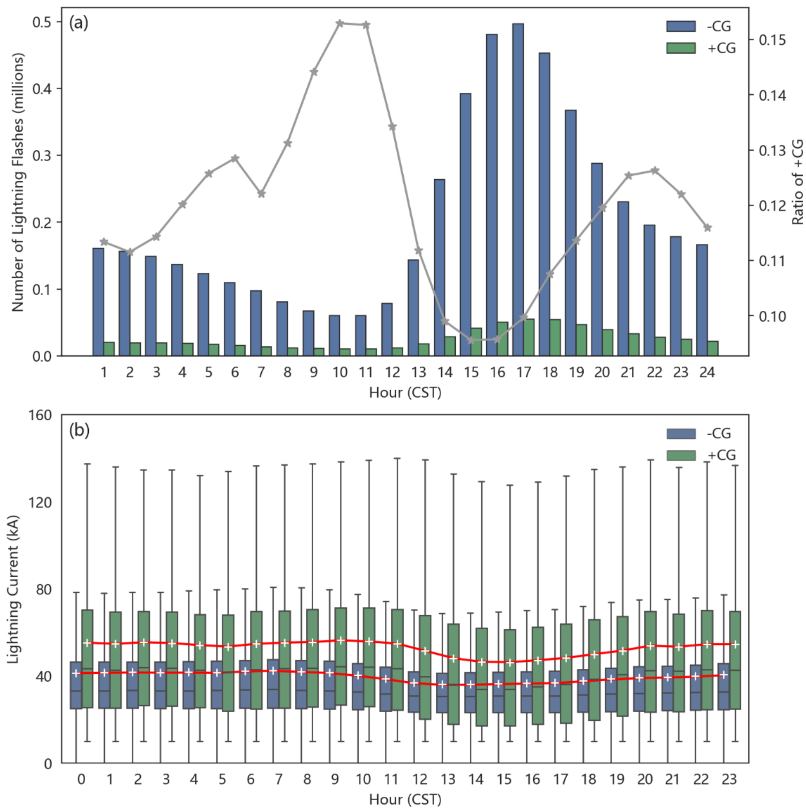

Fig. 8. Daily variation of +CG and -CG (a) flash frequency and (b) discharge intensity.

3.2.2 Comparison of the spatial distribution of +CG and -CG

The geography of China is complex, and the ratio of +CG and -CG flashes have obvious variability in spatial distribution. Fig. 9 shows the spatial distribution of the proportion of +CG flashes. In order to reduce the anomalous values, the grid with less than 10 CG flashes accumulated in 6 years is not included and is indicated in gray. As shown, these grids are mainly distributed in the central, western, and northern parts of the Tibetan and the western and southern parts of the Xinjian. The proportion of +CG flashes in Region-I, where the density of CG flashes is the highest, is low, less than 10%. The other three regions have a higher proportion of +CG, especially the North China Plain and its adjacent Inner Mongolia and parts of Region-III, where the +CG ratio is up to 30-40%. Overall, lower CG density mostly means higher +CG proportion,

https://doi.org/10.5194/nhess-2022-255
Preprint. Discussion started: 14 December 2022
© Author(s) 2022. CC BY 4.0 License.

and high latitude corresponds to high +CG proportion.

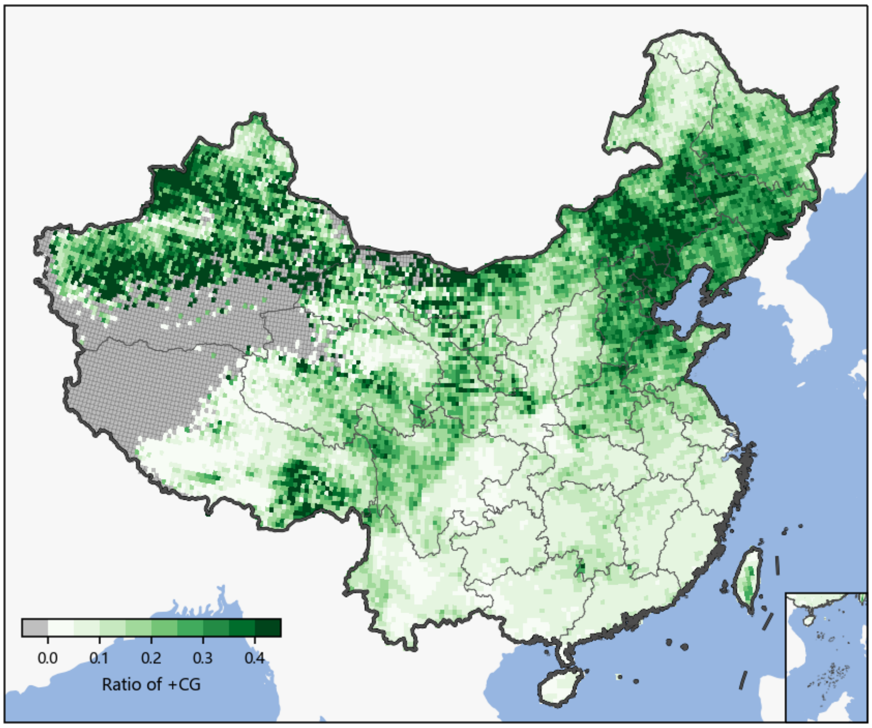

Fig. 9. Distribution of the ratio of +CG flashes in China. The gray grids have a flash number of less than 10 in 6 years and thus are not calculated.

The proportion of +CG flashes in different altitude layers is calculated, as shown by the gray line in Fig. 10. Below 4500 m altitude, the proportion rises with the increase of the altitude, from 7% to 15%. There is a sub-peak at 1500 m, caused by the high ratio region of +CG flashes in Xinjiang and Inner Mongolia. Above 4500 m altitude, which is mainly the uninhabited area in the western and northern Tibetan Plateau, the percentage of +CG decreases rapidly. Only 91 CG flashes occurred above 6000 m altitude in 6 years, so they are not included in the statistics.

The current distribution of +CG and -CG at different altitudes are represented by the box plot in Fig. 10. The distribution of lightning current shrinks with increasing altitude. A fascinating phenomenon is that the average current of -CG flashes is slightly positively correlated with altitude, but +CG flashes are negatively correlated with altitude. The opposite trend of the two causes a large difference in the discharge intensity at low altitudes, but their discharge intensity is close to the same at high altitudes.

https://doi.org/10.5194/nhess-2022-255
Preprint. Discussion started: 14 December 2022
© Author(s) 2022. CC BY 4.0 License.

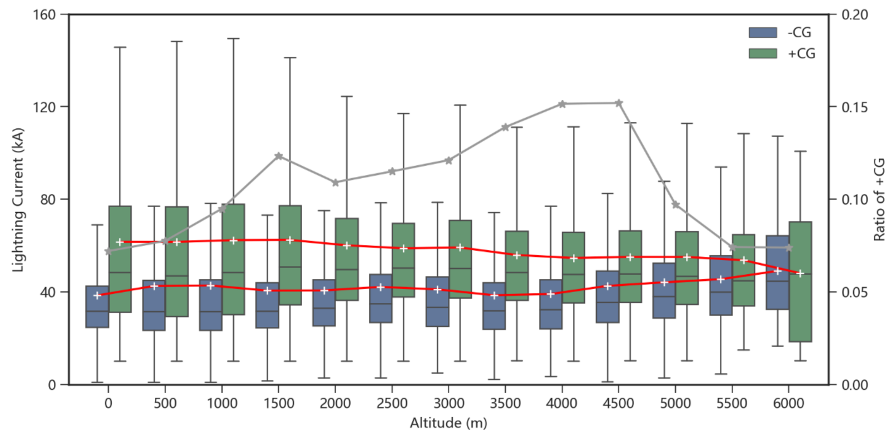

Fig. 10. Relationship between the distribution and altitude of +CG and -CG.

Part of the reason for the complexity of lightning activity in China comes from the Tibetan Plateau, the "third pole" of the Earth, where the charge structure of thunderstorm clouds has some special characteristics due to the high-altitude ground surface. Qie et al. (2002) analyzed the lightning characteristics of thunderstorms on the Tibetan Plateau at an altitude of 1600 m using the lightning location system installed in Pingliang, Gansu, and found that the proportion of +CG flashes is 16% on average, which is higher than that of conventional thunderstorms. Zhang et al. (2007) studied the charge structure of 30 thunderstorms in Nagqu at 4500 m altitude and concluded that although the plateau thunderstorms have a relatively strong lower positive charge region, the lack of a negative charge region that excites the positive charge region to discharge to the ground makes it difficult for +CG to occur. On the contrary, in our study, the proportion of +CG flashes in Nagqu is higher than the average, see Fig. 9. You et al. (2019) analyzed the characteristics of lightning activity in the 18-36°N Asia-Pacific region using lightning imager data from the TRMM satellite. The statistical results showed the discharge intensity of lightning in the Tibetan Plateau is smaller than in other regions at the same latitude. The results of different studies vary, and there is still no clear and unified understanding of the activity characteristics of thunderstorms on the plateau. Further detailed analysis is in demand in combination with topographic and climatic features.

4. Conclusion

China is mainly located in the temperate and subtropical zones, under the combined influence of cold and warm monsoon, the interaction of land and sea, and the undulating terrain. The above factors lead to frequent convective weather combined with abundant lightning activities. Compared with the previous studies on China's nationwide lightning characteristics based on satellite or thunderstorm day observation

https://doi.org/10.5194/nhess-2022-255
Preprint. Discussion started: 14 December 2022
© Author(s) 2022. CC BY 4.0 License.
Natural Hazards and Earth System Sciences
Open Access
EGU
Discussions

from meteorological stations, the lightning location system used in this paper has relatively higher DE and smaller location error for CG lightning.

ADTD and 3D-LLS are two of the three nationwide lightning location systems in China, capable of CG lightning detection. 3D-LLS has an additional function of IC detection. By comparing the observations of the two systems in 2020, it is found that the overall DE of 3D-LLS is about twice that of ADTD. The DE distribution of ADTD is relative uniform, while 3D-LLS has extreme high DE in some parts of Yunnan, Sichuan, Tibet, Inner Mongolia, Hebei, Jilin, etc., where the sites are dense and low DE in central Tibet, western Xinjiang, eastern Qinghai, eastern Heilongjiang, etc., where the sites are scarce. After matching the same radiation sources detected by the two networks, it is found that their detection time difference for the same return stroke is no more than 10 μs, the distance difference is mostly within 2 km, and the current peaks are almost equal. However, the DE of ADTD and 3D-LLS corresponds to only 24.5% and 50.5% of the optical observation in the 3 km radius around the Canton Tower in Guangdong. Besides, 3D-LLS has a high probability of misjudging IC flashes as +CG flashes, leading to the ratio of +CG flashes up to 21.4%, much higher than the ratio (8.5%) of ADTD. The proportion of IC flashes detected by 3D-LLS is only 1/3, which means the DE of IC flashes is still insufficient. Both two systems need to be further improved compared with other international developed networks.

The ADTD dataset for the past six years combined with surface height data is utilized to analyze the CG lightning characteristics on the land of China. In general, more in southern regions than northern regions, more in the mountains than plains at the same latitude, more in humid regions than arid regions, and more in coastal regions than inland regions within the same climate zone. The region with the highest CG flashes density is the southeast coastland. The lowest density is in the northwest deserts and basins and the east and north Tibetan Plateau. The monsoon is the main factor affecting thunderstorms and lightning in southern and northern China, and the Tibetan Plateau leads to the complexity of lightning activity in northwestern China and the Qinghai-Tibet region of China. Nationally, the lightning distribution is consistent with the precipitation on a climatic scale. According to the average CG density of provinces and municipalities, Fujian, Zhejiang, Jiangxi, Guangdong, etc., are in the leading position. The provinces with the lowest density are Xinjiang, Tibet, Gansu, Qinghai, Ningxia, etc.

Due to the different mechanisms of +CG and -CG flashes, their spatial and temporal distribution characteristics differ greatly. In terms of time distribution, lightning activities are most active in summer (70.7%), followed by spring (19.1%) and autumn (9.8%), and scarcest in winter (0.4%). Lightning in spring, autumn, and winter is mainly concentrated in the southeastern coastal areas. In August, when CG lightning is the most frequent, the proportion of +CG is the lowest, less than 10%, and its discharge intensity is weak. In December, with the least lightning number, the proportion of +CG rises to 40%, while the discharge intensity is stronger. Within a day, 17:00 is the peak period of the lightning frequency, and 11:00 is the trough. Similarly,

https://doi.org/10.5194/nhess-2022-255
Preprint. Discussion started: 14 December 2022
© Author(s) 2022. CC BY 4.0 License.

the proportion of +CG is inversely correlated with the lightning frequency, and the discharge intensity of lightning is relatively weak in the afternoon when the lightning is frequent. The +CG and -CG flashes ratio also show evident spatial distribution variability. Southern China, with the highest CG density, has the lowest +CG ratio (less than 10%). The high-latitude regions such as the North China Plain and its adjacent parts of Inner Mongolia and northern and central Xinjiang have a 30-40% ratio. The ratio of +CG below 4500 m is positively correlated with the altitude and decreases rapidly after exceeding 4500 m at the western and northern Tibetan Plateau. The discharge intensity of +CG decreases slightly with the increase of altitude, while that of -CG increases with the altitude. The discharge intensities of the two types have a vast difference at low altitudes and tend to be the same at high altitudes. The above rules have also been verified by the dataset from 3D-LLS.

The lightning location system sites cannot be evenly distributed due to geographic factors, thus bringing about errors in the lightning distribution. The observation from Lightning Mapping Imager (LMI) on the FY-4A satellite will be used to correct the distribution deviations by ground-based data in our following research.

Acknowledgments:

This study is supported by the Key Technologies Research and Development Program of China (2020YFB1600103). We appreciate the Meteorological Observation Centre of CMA and the Institute of Electrical Engineering of CAS for their data support. We also thank the reviewers and editors for their valuable suggestions for this study.

Reference

Bitzer, P. M. and Burchfield, J. C.: Bayesian techniques to analyze and merge lightning locating system data, Geophysical Research Letters, 43, 12,605-612,613, 2016.

Bitzer, P. M., Burchfield, J. C., and Christian, H. J.: A Bayesian Approach to Assess the Performance of Lightning Detection Systems, Journal of Atmospheric & Oceanic Technology, 160115131518002, 2016.

Cummins, K. L., Murphy, M. J., Bardo, E. A., Hiscox, W. L., Pyle, R. B., and Pifer, A. E.: A combined TOA/MDF technology upgrade of the US National Lightning Detection Network, Journal of Geophysical Research: Atmospheres, 103, 9035-9044, 1998.

Jerauld, J., Rakov, V., Uman, M., Rambo, K., Jordan, D., Cummins, K. L., and Cramer, J.: An evaluation of the performance characteristics of the US National Lightning Detection Network in Florida using rocket - triggered lightning, Journal of Geophysical Research: Atmospheres, 110, 2005.

Jiang, R.: Observation and Simulation of CG Lightning Activity Characteristics in the Regions with Tall Structures, University of Chinese Academy of Sciences, 2021.

Ma, R., Zheng, D., Zhang, Y., Yao, W., Zhang, W., and Cuomu, D.: Spatiotemporal Lightning Activity Detected by WWLLN over the Tibetan Plateau and Its Comparison with LIS Lightning, Journal of Atmospheric and Oceanic Technology, 38, 511-523, 2021.

https://doi.org/10.5194/nhess-2022-255
Preprint. Discussion started: 14 December 2022
© Author(s) 2022. CC BY 4.0 License.

Natural Hazards and Earth System Sciences
Discussions

Murphy, M. J. and Said, R. K.: Comparisons of lightning rates and properties from the US National Lightning Detection Network (NLDN) and GLD360 with GOES‐16 Geostationary Lightning Mapper and Advanced Baseline Imager data, Journal of Geophysical Research: Atmospheres, 125, e2019JD031172, 2020.

Nag, A., Rakov, V. A., and Cummins, K. L.: Positive Lightning Peak Currents Reported by the U.S. National Lightning Detection Network, IEEE Transactions on Electromagnetic Compatibility, 56, 404-412, 2014.

Nag, A., Mallick, S., Rakov, V., Howard, J., Biagi, C., Hill, J., Uman, M., Jordan, D., Rambo, K., and Jerauld, J.: Evaluation of US National Lightning Detection Network performance characteristics using rocket‐triggered lightning data acquired in 2004–2009, Journal of Geophysical Research: Atmospheres, 116, 2011.

Poelman, D. R., Honoré, F. o., Anderson, G., and Pedeboy, S.: Comparing a Regional, Subcontinental and Long-Range Lightning Location System over the Benelux and France, Journal of Atmospheric & Oceanic Technology, 30, 2394-2405, 2013.

Pohjola, H. and Mäkelä, A.: The comparison of GLD360 and EUCLID lightning location systems in Europe, Atmospheric research, 123, 117-128, 2013.

Preston and Tolver, S.: The lightning discharge, Philosophical Magazine Series 1, 31, 443-445, 1989.

Qie, X., Yu, Y., Wang, D., WANG, H., and Chu, R.: Characteristics of cloud-to-ground lightning in Chinese inland plateau, Journal of the Meteorological Society of Japan. Ser. II, 80, 745-754, 2002.

Rakov and V., A.: A Review of Positive and Bipolar Lightning Discharges, Amer.metor.soc, 84, 767-776, 2003.

Rakov, V. A. and Uman, M. A.: Lightning: Physics and Effects, Lightning: Physics and Effects2003.

Schulz, W., Diendorfer, G., Pedeboy, S., and Poelman, D. R.: The European lightning location system EUCLID–Part 1: Performance analysis and validation, Natural Hazards and Earth System Sciences, 16, 595-605, 2016.

Srivastava, A., Tian, Y., Qie, X., Wang, D., Sun, Z., Yuan, S., Wang, Y., Chen, Z., Xu, W., and Zhang, H.: Performance assessment of Beijing Lightning Network (BLNET) and comparison with other lightning location networks across Beijing, Atmospheric Research, 197, 76-83, 2017.

Wang, J., Huang, Q., Ma, Q., Chang, S., He, J., Wang, H., Zhou, X., Xiao, F., and Gao, C.: Classification of VLF/LF Lightning Signals Using Sensors and Deep Learning Methods, Sensors (Basel, Switzerland), 20, 2020.

Wu, S., Weitao, L., Qi, Q., Wu, B., Chen, L., Su, Z., Jiang, R., and Zhang, C.: Characteristics of Downward Cloud-to-ground Lightning Flashes Around Canton Tower Based on Optical Observations, Journal of Applied Meteorological Science, 2019.

You, J., Zheng, D., Zhang, Y., Yao, W., and Meng, Q.: Duration, spatial size and radiance of lightning flashes over the Asia-Pacific region based on TRMM/LIS observations, Atmospheric Research, 223, 98-113, 2019.

Zhang, T. L., Xiu-Shu, Q., and Yan, M. H.: The Lightning Characteristics of Thunderstorm over Tibetan Plateau and Its Origin Discussion, Plateau Meteorology, 26, 774-782, 2007.